# Stress intensity factors and interaction of two parallel surface cracks on cylinder under tension

**MK Awang[1], AE Ismail[1],  AL Mohd Tobi[1] and MH Zainulabidin[1]**

[1]Faculty of Mechanical and Manufacturing Engineering, Universiti Tun Hussein Onn Malaysia, Batu Pahat, 86400 Johor, Malaysia.

Email: mdkhair@uthm.edu.my

**Abstract**. This paper presents three-dimensional (3D) finite element solution on multiple surface cracks. The cracks on solid cylinder are similar in sizes, parallel each other, assumed to grow in semi-elliptical shape and subjected to remotely tension loading (mode I). A wide range of parametric study involving crack depth ratios ( $0.1 \leq a/D \leq 0.4$), crack aspect ratios ($0.2 \leq a/b \leq 1.2$), normalized coordinates on crack front ($0.0 \leq x/h \leq 0.93$) and inter-crack distance ratios ($0.005 \leq c/l \leq 0.32$) are considered for numerical estimation of stress intensity factors (SIFs) along crack front. For multiple surface cracks under axial loading, the stress intensity factors along crack front decreased when $c/l$ decreased. When multiple cracks approach one another, the stress intensity changes due to interaction of the stress field. The results show that it produces a stress shielding effects.

Keywords: Stress Intensity Factor, Crack Interaction, Shielding

## 1. Introduction

Cylinders under tension loading are widely used in mechanical and structural engineering. They are normally used as a shaft, rods and so on and frequently subjected to cyclic loadings and tends to fail due to nature of said loadings.  In most cases, multiple cracks are likely initiated due to corrosion [1] and fatigue [2]. Conventional assessments for multiple crack problems are derived from fracture mechanics principle based on single crack configuration. Even by using current design codes, such as BS7910, multiple cracks are usually recharacterized as one larger crack, following certain rules and condition. This may lead to over-conservative and incorrect predictions of the service life of cracked component. On top of that, crack interaction criterion in this failure assessment guideline, are extensively validated by past research work on crack interaction in plate model. However, similar validation based on cylinder model is still lacking.

This paper focused on crack interaction for surface cracks in a cylinder under different crack spacing. The interaction of surface cracks is examined using a calibrated three dimensional finite element procedure, for linear elastic analysis. Crack interactions are evaluated based on the crack

driving force, measured by the stress intensity factor values, determined from an interaction integral approach implemented in a commercial finite element code. The finite element results are validated against available SIF results [3] for cracked cylinder with a single semi-elliptical crack. Despite of availability of efficient techniques and computer to solve three-dimensional crack problems, solution for interactive multiple cracks on cylinder are not much in the literature.

## 2. Review of existing solutions

The problem involved interacting cracks receive increased attention since the last two decade. Chudnovsky et al. [4] have developed different solution techniques that use the method of dislocations. By using the body force method, Murakami and Nemat-Nasser [5] have presented Mode I SIF solutions for a number of interacting coplanar surface cracks in a half-space. These solutions were given for a variety of crack shapes and sizes under tension and bending loads. Using the same technique, Isida et al. [6] studied an array of parallel semi-elliptical surface cracks in a 3D semi-infinite solid under tension. Employing the boundary element method, Tu and Cai[7] have also studied the behavior of 2D non-coplanar cracks contained in an infinite body. Miyazaki et al. [8] used a combined line-spring and boundary element method to obtain mode I solutions for embedded and surface coplanar cracks interacting in a plate. Applying the alternating finite element methods, Stonesifer et al. [9] calculated the SIFs for two symmetric non-coplanar surface cracks interacting in a plate subjected to remote uniaxial tension. Further, classical finite element methods were also used by Jiang et al. [10] to analyze two parallel surface cracks in 3D. In many of the cases studied, the cracks were treated as being symmetric.

## 3. Finite element modelling

The geometry of the crack shown in Figure 1 can be described by the dimensionless parameters *a/D* and *a/b* which are crack depth ratio and crack aspect ratio, respectively. Different crack shapes were considered i.*e a/D* of 0.1, 0.2, 0.3 and 0.4. Meanwhile *a/b* ranging from 0.2 to 1.2 with each increment of 0.2, where the definitions of geometrical parameters agree with those of Shin and Cai [3] and Carpinteri [11]. In this work, there are 14 points along crack front being considered through normalized coordinates *x/h* with special attention given to most outer point, deepest point and one point in between. Only a quarter model are required due to symmetry of the case. The diameter of the cylinder is 50mm and 200mm in length. The Poisson ratio is assumed to be 0.33 and Young's modulus is 70GPa.
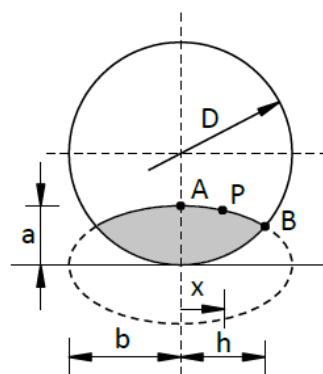


**Figure 1**: Crack characterization [3]

The layout of the problem is shown in Figure 2 where both cracks take place at the middle of the cylinder and the inter-crack distance ratio, *c/l* ranges of 0.005, 0.01, 0.02, 0.04, 0.08, 0.16 and 0.32. Interaction integral method is used to determine the stress intensity factor at the crack front. Since the crack faces are normal to direction of forces, only mode 1 of SIFs is produced. The SIFs are also normalized as below:

$$F_{I,a} = \frac{K_I}{\sigma\sqrt{\pi a}} \qquad\qquad (1)$$

where $K_I$ is the modes I stress intensity factors, while $F_I$ is their corresponding geometrical correction factors or normalized stress intensity factors, $\sigma$ is an axial stress and $a$ is a crack depth.
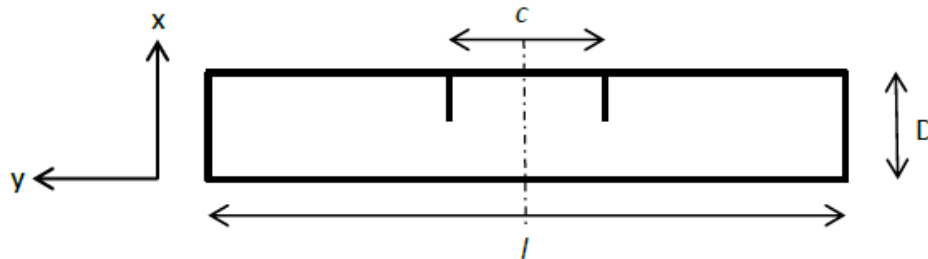


**Figure 2**: The layout of crack

## 4. Results and discussion

**4.1** Stress intensity factors for single crack

In order to employ the appropriate finite element model, it is necessary to compare the proposed model with published data. Figure 3 shows a comparison of the SIFs values of a single crack under tension loading as well as those predicted by Shin and Cai [3]. It is found that the results are in a good agreement. Therefore, the proposed model can be used with confident to determine the SIF values of multiple cracks.
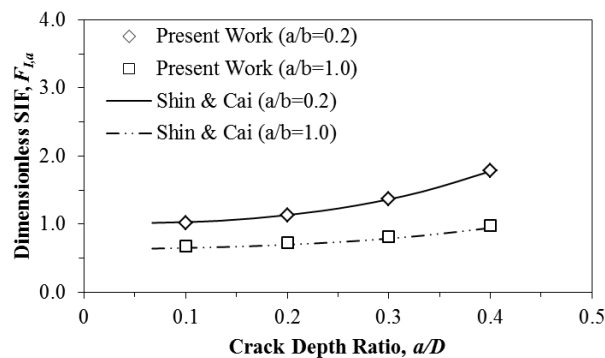


**Figure 3**: Validation of present model

**4.2** Double crack interaction

Schematic diagram of the interactive cracks is shown in Figure 2. The cylinder is subjected to a remote tension load in $y$-direction. A finite element model is developed using ANSYS Parametric Design Language (APDL) code and parallel interacting surface crack are modelled using 20-noded isoparametric quadratic brick elements. The interaction process is quantified by calculating the interaction factor, $\gamma$ which is defined by ratio of normalized SIF between a cylinder with two cracks and a cylinder with a single crack. Since the problem is symmetrical, only a quarter of cylinder has been modelled. Wide ranges of crack configuration, i.e $(0.1 \leq a/D \leq 0.4)$, $(0.2 \leq a/b \leq 1.2)$, $(0.0 \leq x/h \leq 0.93)$ and $(0.005 \leq c/l \leq 0.32)$ have been analyzed and the results are displayed both in graphical and tabular forms.

Figures 4 – 7 show the variation of SIF along crack front for various inter-crack distance when the crack aspect ratio, $a/b$ is kept constant at 0.6. It is apparent that various inter-crack distance produce

shielding effect rather than amplification effect. The closer the two cracks are, the greater the interaction is, the stress field is relaxed thus the more the dimensionless SIF decreases. The same pattern goes for the rest of crack aspect ratio. The dimensionless SIF values almost identical with single crack when $c/l$ reaches 0.32. This means there is no more interaction beyond this ratio and two interacting crack can be treated as a single separate crack. It can be seen that the plotted graph in Figure 7 have more gap each other than Figure 4 which indicates the dimensionless SIF not only depends on $c/l$. In this regards, $a/D$ plays a significant roles. The dimensionless SIF always achieve its maximum at outer point ($x/h$ = 0.93). This is due to state of stress changes slowly from plain strain at deepest point to plain stress at outer point. Therefore, to estimate the critical load for any crack propagation, determination of the stress intensity factor at the free surface of the cylinder is the most crucial.
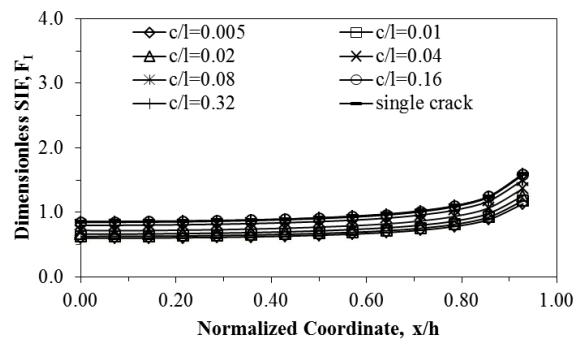


**Figure 4**: The variatons of SIF along crack front for various intercrack distance, $c/l$ when $a/D$= 0.1, $a/b$=0.6
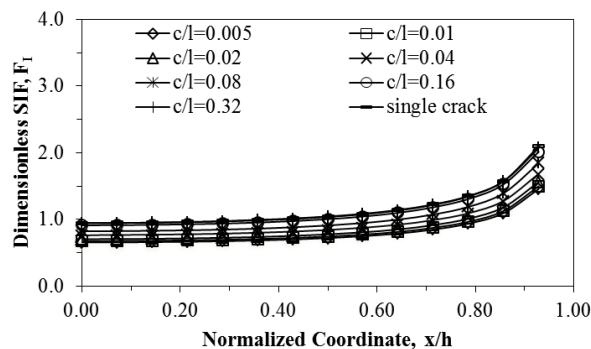


**Figure 5**: The variatons of SIF along crack front for various intercrack distance, $c/l$ when $a/D$= 0.2, $a/b$=0.6
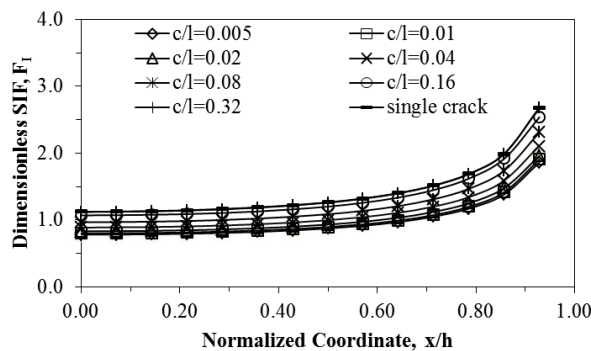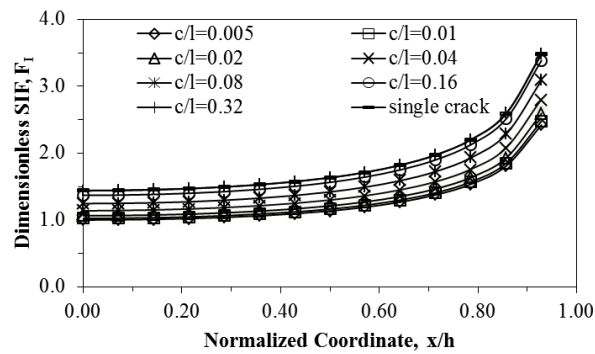


**Figure 6**: The variatons of SIF along crack front for various intercrack distance, $c/l$ when $a/D$= 0.3, $a/b$=0.6

**Figure 7**: The variatons of SIF along crack front for various intercrack distance, *c/l* when *a/D*= 0.4, *a/b*=0.6
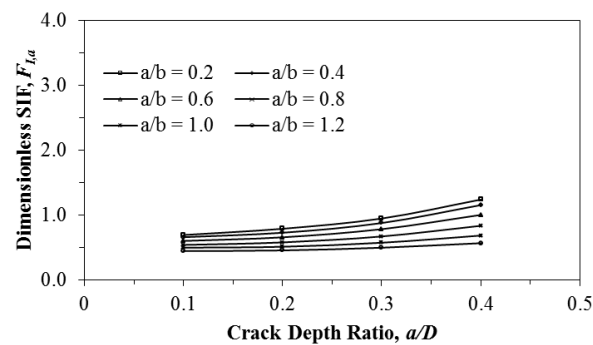


**Figure 8** : Dimensionless SIF vs *a/D* at deepest point when *c/l*=0.005

To further investigate the normalised SIF effect due to the size of cracks, parametric study with varying *a/D* and *a/b* is carried out. Figure 8 shows the variation of the normalised SIFs with respect to crack depth ratio, *a/D*. The latter plays a significant role at lower *a/b* but less effect at *a/b*=1.2. Meanwhile, *a/b* between 0.4-0.8 has a biggest effect on value of normalised SIF as shown in Fig 9.
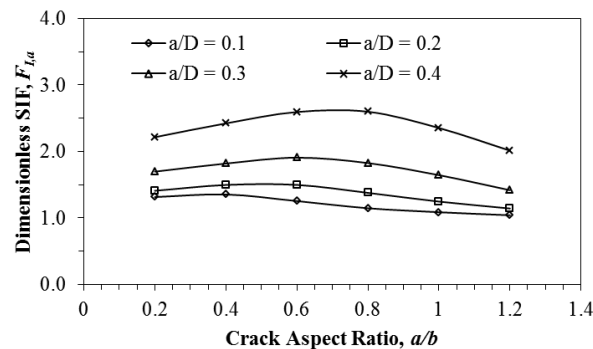


**Figure 9** : Dimensionless SIF vs *a/b* at outer point when *c/l*=0.02

Tables 1 – 6 show the variation of interaction factor, measured at three different locations along crack front. These point represent deepest point *x/h*=0, outer point *x/h*=0.93 and *x/h*=0.5. It is noted that the values of *γ* always less than unity, which serves as a reference as it represents the magnification or shielding effects. Then only when *c/l* approaches 0.32, there is no more shielding effect at all locations along crack front. The maximum reduction of 33% in interaction factor occurs when *a/b*=0.2, *a/D*=0.1 at deepest point. The variations in the values of *γ* can be compared with the variations of normalized SIF.

**Table 1**: Interaction factor for two parallel surface cracks under tension when *a/b* = 0.2

|     |     | c/L |     |     |     |     |     |     |
|-----|-----|-----|-----|-----|-----|-----|-----|-----|
| **a/D** | **x/h** | 0.005 | 0.01 | 0.02 | 0.04 | 0.08 | 0.16 | 0.32 |
|     | 0.00 | 0.67 | 0.71 | 0.75 | 0.80 | 0.89 | 0.97 | 0.99 |
| 0.1 | 0.50 | 0.66 | 0.70 | 0.74 | 0.81 | 0.89 | 0.95 | 0.99 |
|     | 0.93 | 0.75 | 0.80 | 0.86 | 0.92 | 0.96 | 0.99 | 1.00 |
|     |      |      |      |      |      |      |      |      |
|     | 0.00 | 0.69 | 0.71 | 0.73 | 0.78 | 0.86 | 0.96 | 1.00 |
| 0.2 | 0.50 | 0.70 | 0.72 | 0.74 | 0.79 | 0.87 | 0.97 | 1.00 |
|     | 0.93 | 0.71 | 0.74 | 0.78 | 0.85 | 0.93 | 0.98 | 1.00 |
|     |      |      |      |      |      |      |      |      |
|     | 0.00 | 0.69 | 0.71 | 0.74 | 0.78 | 0.86 | 0.95 | 1.00 |
| 0.3 | 0.50 | 0.69 | 0.71 | 0.74 | 0.79 | 0.86 | 0.96 | 1.00 |
|     | 0.93 | 0.70 | 0.73 | 0.77 | 0.83 | 0.92 | 0.99 | 1.00 |
|     |      |      |      |      |      |      |      |      |
|     | 0.00 | 0.69 | 0.71 | 0.74 | 0.79 | 0.87 | 0.95 | 1.00 |
| 0.4 | 0.50 | 0.69 | 0.71 | 0.74 | 0.79 | 0.87 | 0.96 | 1.00 |
|     | 0.93 | 0.70 | 0.72 | 0.76 | 0.82 | 0.91 | 0.99 | 1.00 |

**Table 2**: Interaction factor for two parallel surface cracks under tension when *a/b* = 0.4

|     |     | c/L |     |     |     |     |     |     |
|-----|-----|-----|-----|-----|-----|-----|-----|-----|
| **a/D** | **x/h** | 0.005 | 0.01 | 0.02 | 0.04 | 0.08 | 0.16 | 0.32 |
|     | 0.00 | 0.69 | 0.72 | 0.76 | 0.82 | 0.91 | 0.98 | 0.99 |
| 0.1 | 0.50 | 0.69 | 0.73 | 0.77 | 0.83 | 0.92 | 0.98 | 1.00 |
|     | 0.93 | 0.73 | 0.77 | 0.83 | 0.89 | 0.96 | 1.00 | 1.00 |
|     |      |      |      |      |      |      |      |      |
|     | 0.00 | 0.69 | 0.71 | 0.74 | 0.79 | 0.86 | 0.96 | 1.00 |
| 0.2 | 0.50 | 0.69 | 0.71 | 0.74 | 0.79 | 0.87 | 0.96 | 1.00 |
|     | 0.93 | 0.70 | 0.73 | 0.78 | 0.84 | 0.91 | 0.98 | 1.00 |
|     |      |      |      |      |      |      |      |      |
|     | 0.00 | 0.69 | 0.71 | 0.74 | 0.79 | 0.86 | 0.95 | 1.00 |
| 0.3 | 0.50 | 0.69 | 0.71 | 0.74 | 0.79 | 0.86 | 0.95 | 1.00 |
|     | 0.93 | 0.69 | 0.72 | 0.76 | 0.82 | 0.90 | 0.95 | 1.00 |
|     |      |      |      |      |      |      |      |      |
|     | 0.00 | 0.70 | 0.71 | 0.74 | 0.79 | 0.87 | 0.96 | 1.00 |
| 0.4 | 0.50 | 0.69 | 0.72 | 0.74 | 0.80 | 0.87 | 0.96 | 1.00 |
|     | 0.93 | 0.70 | 0.72 | 0.76 | 0.82 | 0.91 | 0.99 | 1.00 |

**Table 3**: Interaction factor for two parallel surface cracks under tension when *a/b* = 0.6

|     |     | c/L |     |     |     |     |     |     |
|-----|-----|-----|-----|-----|-----|-----|-----|-----|
| **a/D** | **x/h** | 0.005 | 0.01 | 0.02 | 0.04 | 0.08 | 0.16 | 0.32 |
|     | 0.00 | 0.70 | 0.73 | 0.77 | 0.84 | 0.93 | 0.98 | 0.99 |
| 0.1 | 0.50 | 0.70 | 0.73 | 0.78 | 0.85 | 0.93 | 0.99 | 0.99 |
|     | 0.93 | 0.71 | 0.74 | 0.79 | 0.86 | 0.94 | 0.99 | 1.00 |
|     |      |      |      |      |      |      |      |      |
|     | 0.00 | 0.69 | 0.71 | 0.75 | 0.80 | 0.87 | 0.96 | 1.00 |
| 0.2 | 0.50 | 0.69 | 0.71 | 0.74 | 0.79 | 0.87 | 0.96 | 0.99 |
|     | 0.93 | 0.69 | 0.71 | 0.74 | 0.80 | 0.88 | 0.96 | 0.99 |
|     |      |      |      |      |      |      |      |      |
|     | 0.00 | 0.69 | 0.71 | 0.74 | 0.79 | 0.86 | 0.95 | 1.00 |
| 0.3 | 0.50 | 0.69 | 0.71 | 0.74 | 0.79 | 0.86 | 0.95 | 1.00 |
|     | 0.93 | 0.69 | 0.71 | 0.73 | 0.78 | 0.86 | 0.95 | 1.00 |
|     |      |      |      |      |      |      |      |      |
|     | 0.00 | 0.69 | 0.71 | 0.74 | 0.79 | 0.86 | 0.95 | 1.00 |
| 0.4 | 0.50 | 0.70 | 0.71 | 0.74 | 0.79 | 0.87 | 0.96 | 1.00 |
|     | 0.93 | 0.70 | 0.71 | 0.75 | 0.80 | 0.89 | 0.97 | 1.00 |

**Table 4**: Interaction factor for two parallel surface cracks under tension when *a/b* = 0.8

| a/D | x/h | c/L 0.005 | 0.01 | 0.02 | 0.04 | 0.08 | 0.16 | 0.32 |
|---|---|---|---|---|---|---|---|---|
| | 0.00 | 0.70 | 0.74 | 0.79 | 0.86 | 0.94 | 0.98 | 0.99 |
| 0.1 | 0.50 | 0.71 | 0.74 | 0.79 | 0.86 | 0.94 | 0.99 | 0.99 |
| | 0.93 | 0.69 | 0.72 | 0.77 | 0.85 | 0.94 | 0.99 | 1.00 |
| | 0.00 | 0.69 | 0.72 | 0.75 | 0.81 | 0.88 | 0.97 | 0.99 |
| 0.2 | 0.50 | 0.70 | 0.72 | 0.75 | 0.81 | 0.88 | 0.97 | 1.00 |
| | 0.93 | 0.69 | 0.71 | 0.74 | 0.80 | 0.88 | 0.97 | 1.00 |
| | 0.00 | 0.69 | 0.71 | 0.74 | 0.79 | 0.87 | 0.95 | 1.00 |
| 0.3 | 0.50 | 0.69 | 0.71 | 0.74 | 0.79 | 0.87 | 0.95 | 1.00 |
| | 0.93 | 0.69 | 0.71 | 0.74 | 0.79 | 0.86 | 0.96 | 1.00 |
| | 0.00 | 0.69 | 0.71 | 0.74 | 0.79 | 0.87 | 0.95 | 1.00 |
| 0.4 | 0.50 | 0.70 | 0.71 | 0.74 | 0.79 | 0.87 | 0.95 | 1.00 |
| | 0.93 | 0.69 | 0.70 | 0.74 | 0.79 | 0.87 | 0.96 | 1.00 |

**Table 5**: Interaction factor for two parallel surface cracks under tension when *a/b* = 1.0

| a/D | x/h | c/L 0.005 | 0.01 | 0.02 | 0.04 | 0.08 | 0.16 | 0.32 |
|---|---|---|---|---|---|---|---|---|
| | 0.00 | 0.73 | 0.75 | 0.81 | 0.88 | 0.96 | 0.99 | 0.99 |
| 0.1 | 0.50 | 0.73 | 0.75 | 0.80 | 0.88 | 0.96 | 0.99 | 1.00 |
| | 0.93 | 0.72 | 0.72 | 0.77 | 0.86 | 0.95 | 0.99 | 1.00 |
| | 0.00 | 0.70 | 0.72 | 0.76 | 0.82 | 0.90 | 0.97 | 1.00 |
| 0.2 | 0.50 | 0.70 | 0.72 | 0.76 | 0.82 | 0.90 | 0.97 | 1.00 |
| | 0.93 | 0.69 | 0.71 | 0.74 | 0.79 | 0.88 | 0.98 | 1.00 |
| | 0.00 | 0.70 | 0.72 | 0.75 | 0.80 | 0.88 | 0.96 | 1.00 |
| 0.3 | 0.50 | 0.70 | 0.72 | 0.75 | 0.80 | 0.87 | 0.96 | 1.00 |
| | 0.93 | 0.70 | 0.71 | 0.73 | 0.78 | 0.85 | 0.95 | 1.00 |
| | 0.00 | 0.70 | 0.72 | 0.74 | 0.79 | 0.87 | 0.96 | 1.00 |
| 0.4 | 0.50 | 0.70 | 0.72 | 0.75 | 0.80 | 0.87 | 0.96 | 1.00 |
| | 0.93 | 0.70 | 0.71 | 0.74 | 0.78 | 0.86 | 0.95 | 1.00 |

**Table 6**: Interaction factor for two parallel surface cracks under tension when *a/b* = 1.2

| a/D | x/h | c/L 0.005 | 0.01 | 0.02 | 0.04 | 0.08 | 0.16 | 0.32 |
|---|---|---|---|---|---|---|---|---|
| | 0.00 | 0.73 | 0.76 | 0.83 | 0.90 | 0.97 | 0.99 | 0.99 |
| 0.1 | 0.50 | 0.72 | 0.75 | 0.82 | 0.90 | 0.97 | 1.00 | 1.00 |
| | 0.93 | 0.68 | 0.72 | 0.78 | 0.87 | 0.96 | 0.99 | 1.00 |
| | 0.00 | 0.70 | 0.73 | 0.78 | 0.84 | 0.92 | 0.98 | 1.00 |
| 0.2 | 0.50 | 0.70 | 0.73 | 0.77 | 0.83 | 0.91 | 0.98 | 1.00 |
| | 0.93 | 0.70 | 0.71 | 0.73 | 0.79 | 0.89 | 0.98 | 1.00 |
| | 0.00 | 0.70 | 0.72 | 0.76 | 0.82 | 0.90 | 0.97 | 1.00 |
| 0.3 | 0.50 | 0.70 | 0.72 | 0.75 | 0.81 | 0.89 | 0.97 | 1.00 |
| | 0.93 | 0.69 | 0.69 | 0.72 | 0.78 | 0.85 | 0.96 | 1.00 |
| | 0.00 | 0.70 | 0.72 | 0.75 | 0.80 | 0.88 | 0.96 | 1.00 |
| 0.4 | 0.50 | 0.70 | 0.72 | 0.75 | 0.80 | 0.88 | 0.96 | 1.00 |
| | 0.93 | 0.70 | 0.71 | 0.73 | 0.78 | 0.85 | 0.95 | 1.00 |

Figure 10 shows the interaction factor along crack front. It can be seen that there is a slight increase of interaction factor as graph approaches outer point for the most of the considered cases. On the other hand, there are the cases where the interaction is higher at outer point. In other words, the location on crack front does not show the significant effect on interaction factor as far as parallel crack is concern. Unless the crack configuration is different which is interesting to be investigates.
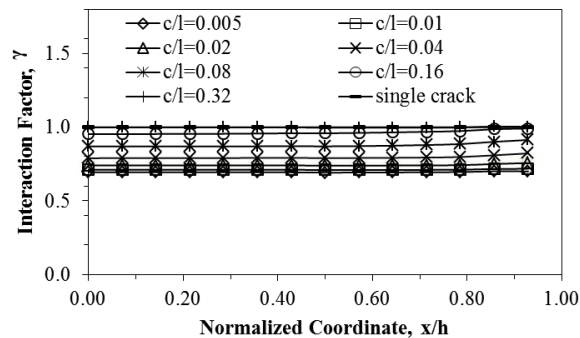
**Figure 10**: Interaction factors along crack front *at a/D* = 0.4*, a/b* = 0.2

## 5. Conclusions

Based on the investigations conducted numerically using ANSYS finite element program on the parallel cracks subjected to tension stress, the following remarks are drawn from this study:-

1. As expected, higher crack depth ratio produced higher SIFs for mode 1 stress intensity factors.
2. The maximum SIF always occurs at outer point on crack front. This is due to state of stress changes gradually from plain strain at deepest point to plain stress.
3. When there is two parallel interacting cracks, the flexibility of cylinder increases, the SIF decrease.
4. The interaction diminishes along with the increase of inter-crack distance.

## References

[1]  Leis BN 1997 *Proceedings of the Seventh ISOPE, Vol. 4, Quebec, Canada* pp. 607–613.
[2]  Soboyejo WO, Knott JF 1990 *Eng. Fracture Mech.* 37:323–340.
[3]  Shin CS, Cai CQ 2004. *Int Journal of Fracture* 129:239–64.
[4]  Chudnovsky A, Dolgopolsky A, Kachanov M 1987. *Int. J. Solids Structures* 23:1–10.
[5]  Murakami Y, Nemat-Nasser S. 1982 *Eng. Fracture Mech* 16:373–386.
[6]  Isida M, Yoshida T, Noguchi H.1991. *Eng. Fracture Mech.* 39:845–850.
[7]  Tu ST, Cai RY. 1988 *Computational Mechanics Publications*, pp. 239–247.
[8]  Miyazaki H, Kaneko H, Murakata T.1989. *Int. J. Press. Vess. Piping* 38:1–14.
[9]  Stonesifer RB, Brust FW, Leis BN. 1993 *Eng. Fracture Mech.* 45:357–380.
[10] Jiang ZD, Petit J, Akid R, Bezine G. 1991 *Eng. Fracture Mech.* 40:345–354.
[11] Carpinteri A. 1992 *Fatigue Fract Eng Mater Struct* 15(11):1141–53.